

Supplement of Earth Syst. Dynam., 8, 865–873, 2017  
<https://doi.org/10.5194/esd-8-865-2017-supplement>  
© Author(s) 2017. This work is distributed under  
the Creative Commons Attribution 3.0 License.



*Supplement of*

## **Climatology of Lyapunov exponents: the link between atmospheric rivers and large-scale mixing variability**

**Daniel Garaboa-Paz et al.**

*Correspondence to:* Vicente Pérez-Muñuzuri ([vicente.perez@cesga.es](mailto:vicente.perez@cesga.es))  
and Daniel Garaboa-Paz ([angeldaniel.garaboa@usc.es](mailto:angeldaniel.garaboa@usc.es))

The copyright of individual parts of the supplement might differ from the CC BY 3.0 License.

### Seasonal effects on the FTLE climatology

Figures 1,2 account for the seasonal effect observed in the FTLE climatology for the period 1979 – 2014. Note the largest values of the FTLE alternate between southern and northern hemispheres along the whole period. As observed in Figure 1 in the main text, three latitudinal bands are also clearly visible in the Hovmöller diagram. Note that the maximum values are observed for mid-latitudes.

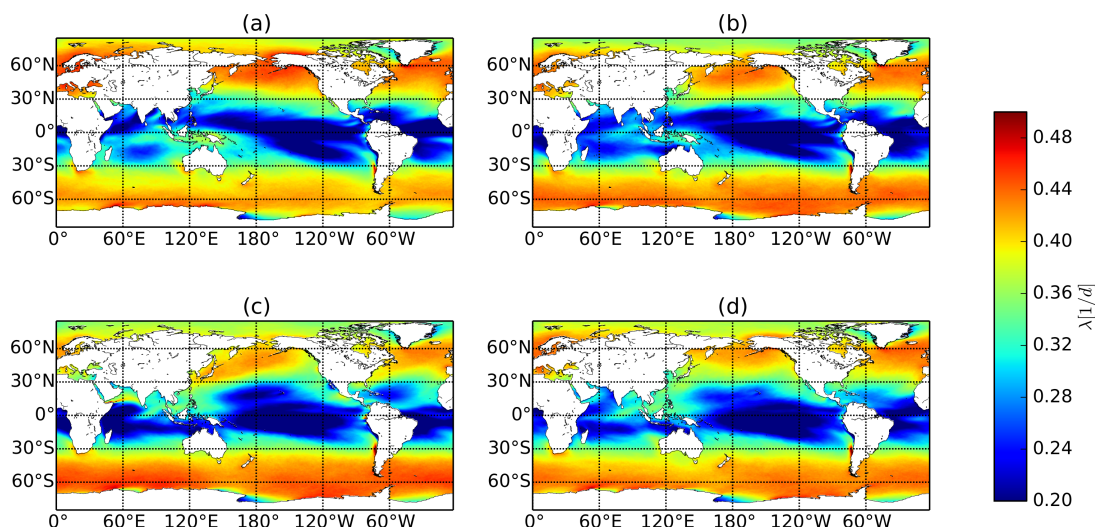


**Figure 1.** Seasonal mean for the backward FTLE based on the 35 years timeseries for the seasonal periods; (a) DJF, (b) MAM, (c) JJA, and (d) SON. Note the largest values of the FTLE for the northern/southern hemisphere during the winter season.

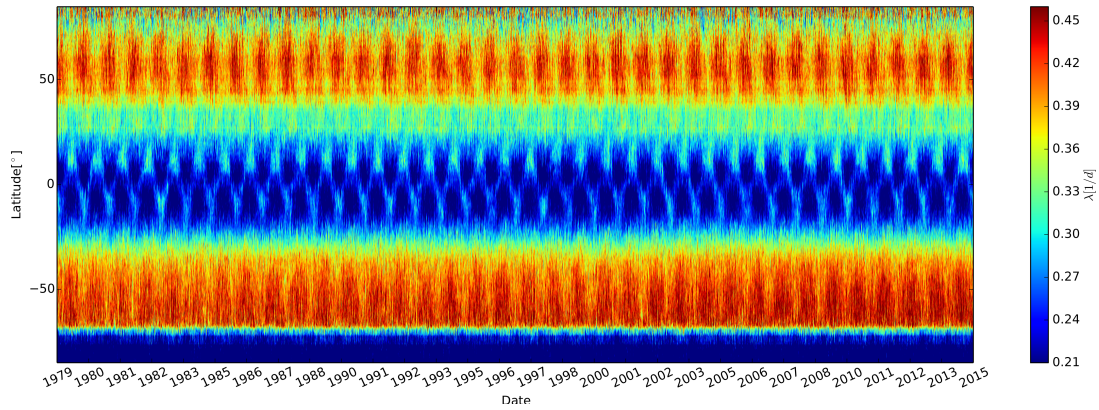


**Figure 2.** Hovmöller diagram based on week averages for the 35 years FTLE backward timeseries.

### Correlation between the FTLE time series and ENSO indices

Figure 3 shows the monthly backward and forward FTLE time series and the Southern Oscillation Index (SOI) for the 1979-2014 period. The FTLE series are anticorrelated with the SOI index, with correlation coefficients  $-0.85$  and  $-0.67$ , respectively.

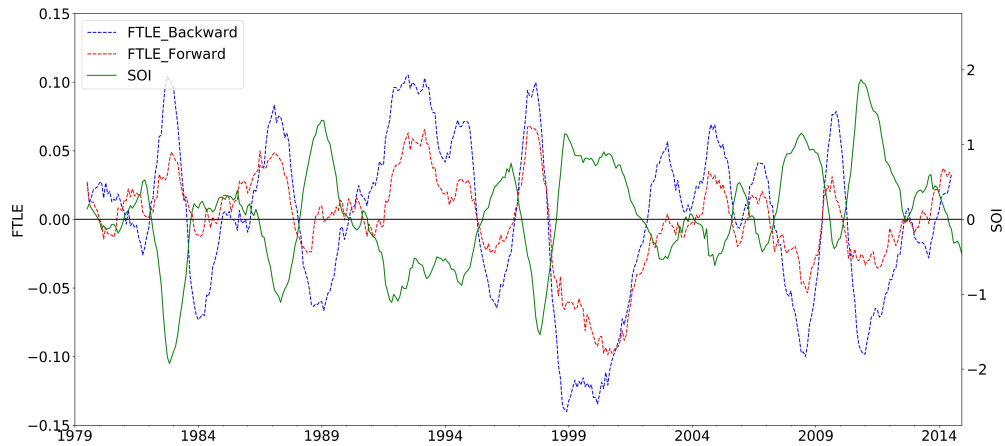


**Figure 3.** Monthly time evolution of the backward/forward FTLE anomalies and the SOI Index for the 1979-2014 period.

## 5 Precipitation rates in Sahara and British Isles due to Atmospheric Rivers

Figure 4 shows the rainfall rates measured in the Sahara-Morocco (a) and British Isles (b) regions coinciding with a landfall atmospheric river. Precipitation rates are shown as a percentage out of the total retrieved from *Sheffield et al. (2005)*.

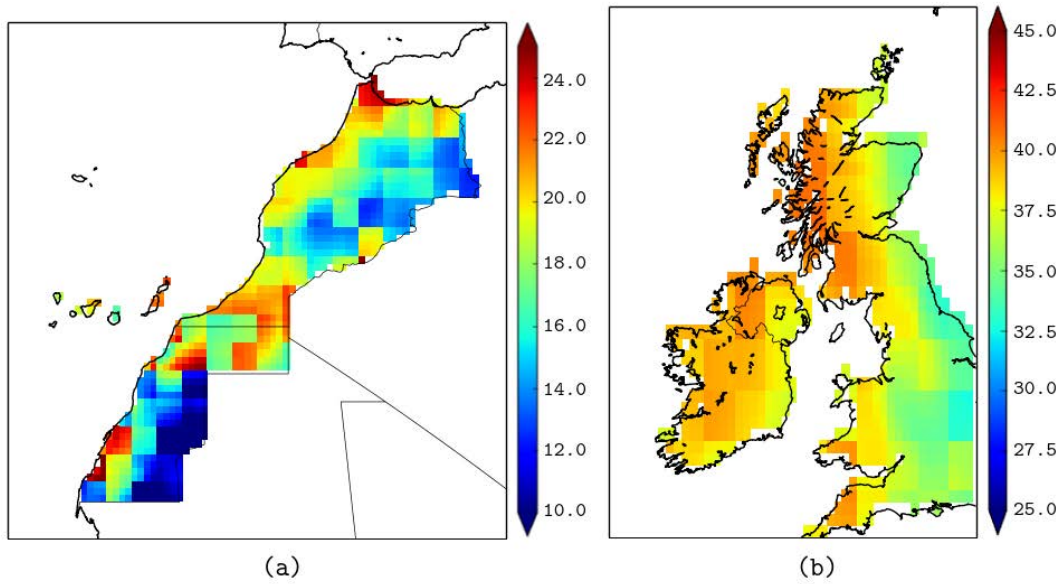


**Figure 4.** Ratio of daily precipitation coinciding with an atmospheric river detection out of the total, for the Sahara-Morocco (a) and UK-Ireland (b) regions. The database of precipitation used in this analysis is the global rain data retrieved from *Sheffield et al. (2005)*. This global high-resolution dataset has been constructed by the combination of observational and reanalysis data from the NCEP-NCAR.

## References

Sheffield, J., G. Goteti, and E.F. Wood (2006). Development of a 50-year high-resolution global dataset of meteorological forcings for land surface modeling. *Journal of Climate*, 19(13), 3088–3111, doi:10.1175/JCLI3790.1.